

# A TABLE OF $n$ -COMPONENT HANDLEBODY LINKS OF GENUS $n + 1$ UP TO SIX CROSSINGS

GIOVANNI BELLETTINI, GIOVANNI PAOLINI, MAURIZIO PAOLINI,  
AND YI-SHENG WANG

ABSTRACT. A handlebody link is a union of handlebodies of positive genus embedded in 3-space, which generalizes the notion of links in classical knot theory. In this paper, we consider handlebody links with one genus 2 handlebody and  $n - 1$  solid tori,  $n > 1$ . Our main result is the complete classification of such handlebody links with six crossings or less, up to ambient isotopy.

## 1. INTRODUCTION

Knot tabulation has a long and rich history. Some early work, motivated by Kelvin's vortex theory, dates back to as early as the late 19th. Over the past decades, more effort has been put into it by many physicists and mathematicians; all prime knots up to 16 crossings are now classified [8]. In recent years knot tabulation has been further generalized to other contexts. [17] and [19] tabulate all prime theta curves and handcuff graphs up to seven crossings, [10] enumerates all irreducible handlebody knots of genus 2 up to six crossings, and [5] classifies all alternating Legendrian knots up to seven crossings.

The aim of this paper is to extend the Ishii-Kishimoto-Moriuchi-Suzuki handlebody knot table [10] to handlebody *links* with  $n > 1$  components having total genus  $n + 1$ . We call such a handlebody link an  $(n, 1)$ -handlebody link; it consists of exactly one genus 2 handlebody and  $n - 1$  solid tori. The following theorems summarize the main results of the paper.

**Theorem 1.1.** *Table 1 enumerates all non-split<sup>1</sup>, irreducible<sup>2</sup>  $(n, 1)$ -handlebody links, up to ambient isotopy and mirror image, by their minimal diagrams, up to six crossings.*

$4_1$  and  $5_1$  in Table 1 are the only non-split, irreducible  $(n, 1)$ -handlebody links with four and five crossings, respectively. There are 15 handlebody links with six crossings, among which 8 have two components ( $n = 2$ ), 6 have three components ( $n = 3$ ), and 1 has four components ( $n = 4$ ). As a side note,  $6_5$  in Table 1 also represents the famous *figure eight puzzle* devised by Stewart Coffin [3]. Thus, its unspittability implies the impossibility of solving the puzzle (Remark 3.2). Also,  $6_9$  in Table 1 is an irreducible handlebody link with a  $\partial$ -irreducible complement; such phenomenon cannot happen when  $n = 1$  (Remark 3.3).

Our task with respect to Table 1 is two-fold. Firstly we need to show that there is no extraneous entry, i.e. that all entries in the table

- U.1 represent non-split handlebody links,
- U.2 represent irreducible handlebody links,

---

*Date:* March 24, 2020.

<sup>1</sup>A handlebody link HL is split if there is a 2-sphere  $\mathfrak{S} \subset \mathbb{S}^3$  with  $\mathfrak{S} \cap \text{HL} = \emptyset$  separating HL into two parts.

<sup>2</sup>A handlebody link HL is reducible if there is a 2-sphere  $\mathfrak{S}$  in  $\mathbb{S}^3$  with  $\mathfrak{S} \cap \text{HL}$  an incompressible disk in HL.

U.3 are mutually inequivalent, up to mirror image,  
 U.4 attain minimal crossing numbers.

Secondly we have to prove that the table is *complete*; namely, there is no missing handlebody link with 6 crossings or less.

In Section 3 we prove U.1-U.3, making use of invariants such as the linking number [16], irreducibility criteria [2], and the Kitano-Suzuki invariant [13] (Theorems 3.2, 3.7, and 3.1, respectively). We prove the completeness of Table 1 by exhausting all—except for those obviously non-minimal—diagrams of non-split, irreducible  $(n, 1)$ -handlebody links up to six crossings (Section 4).

We first observe that the underlying plane graph of a diagram of a non-split, irreducible  $(n, 1)$ -handlebody link necessarily has edge connectivity equal to 2 or 3; for the sake of simplicity, such a diagram is said to have 2- or 3-connectivity, respectively. Diagrams with 3-connectivity up to six crossings are generated by a computer code, whereas to recover handlebody links represented by diagrams with 2-connectivity, we employ the knot sum—the *order-2 vertex connected sum*—of spatial graphs [17]. In more detail, a minimal diagram  $D$  with 2-connectivity can be decomposed by decomposing circles<sup>3</sup> into simpler tangle diagrams, each of which induces a spatial graph that admits a minimal diagram with 3- or 4-connectivity, as illustrated in Fig. 1.1. This decomposition allows us to recover the handlebody link represented by  $D$  by performing the *knot sum* between prime links and a *spatial graph* that admits a minimal diagram with 3-connectivity.

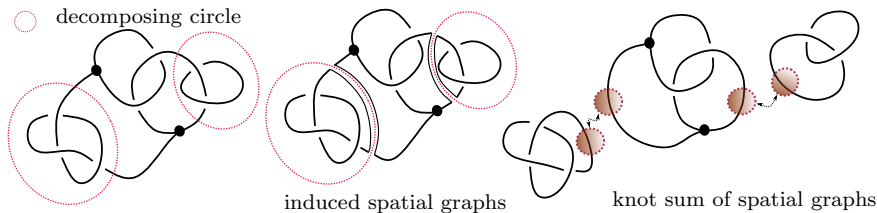


FIGURE 1.1. Decomposing a minimal diagram with 2-connectivity.

Once a list containing all possible minimal diagrams of non-split, irreducible handlebody links is produced, we examine each entry on the list manually (Appendix A), and show that either it is non-minimal or it represents a handlebody link ambient isotopic to one in Table 1, up to mirror image. This proves the completeness, and also implies U.4, given U.1-U.3.

**Theorem 1.2.** *All but  $5_1, 6_3, 6_6, 6_7, 6_8, 6_{10}$  in Table 1 are achiral.*

The main tool used to inspect chirality is Theorem 5.3, where we prove a uniqueness result for the decomposition of non-split, irreducible handlebody links in terms of order-2 connected sum of handlebody-link-disk pairs (Definition 5.1).

**Theorem 1.3.** *Table 5 enumerates all non-split, reducible  $(n, 1)$ -handlebody links up to 6 crossings, up to mirror image.*

Theorem 1.3 follows from the irreducibility of handlebody links in Table 1 and a uniqueness factorization theorem (Theorem 6.1) for non-split, reducible  $(n, 1)$ -handlebody links in terms of order-1 connected sum (Definition 6.1).

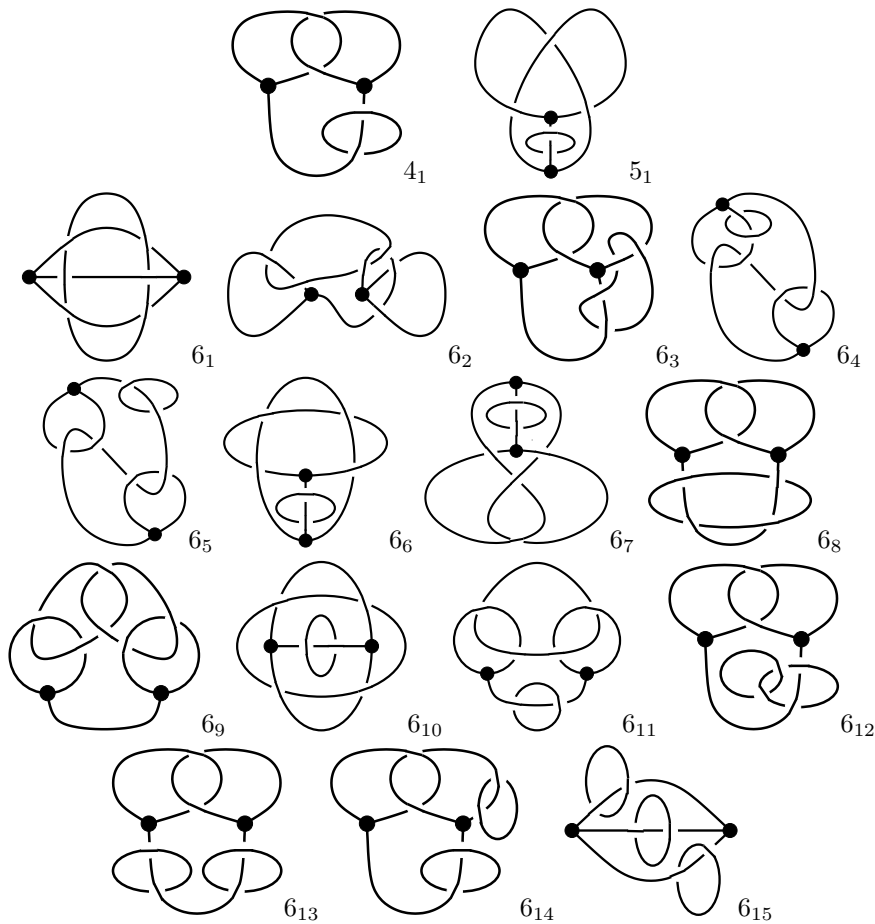
The structure of the paper is the following. Basic properties of handlebody links are reviewed in Section 2; uniqueness, unsplittability, and irreducibility of handlebody links in Table 1 are examined in Section 3. The completeness of the

<sup>3</sup>a circle that intersects  $D$  at two different arcs.

table is discussed in Section 4. Section 5 introduces the notion of decomposable handlebody links, which is used for examining the chirality of handlebody links in Table 1. Lastly, a complete classification of non-split, reducible handlebody links, up to 6 crossings, is given in Section 6. In the appendix we include an analysis on the output of the code, available at <http://dmf.unicatt.it/paolini/handlebodylinks/>.

Throughout the paper we work in the PL category; for the illustrative purposes, the drawings often appear smooth. In the case of 3-dimensional submanifolds in  $\mathbb{S}^3$ , the PL category is equivalent to the smooth category due to [4, Theorem 5], [7, Theorems 7.1, 7.4], [20, Theorem 8.8, 9.6, 10.9].

TABLE 1. Non-split, irreducible handlebody links up to six crossings.



## 2. PRELIMINARIES

### 2.1. Handlebody links and spatial graphs.

**Definition 2.1 (Embeddings in  $\mathbb{S}^3$ ).** *A handlebody link HL (resp. a spatial graph  $G$ ) is an embedding of finitely many handlebodies of positive genus (resp. a finite graph<sup>4</sup>) in the oriented 3-sphere  $\mathbb{S}^3$ .*

<sup>4</sup>A finite graph is a graph with finitely many vertices and edges; in addition, we require that no component has a positive Euler characteristic, to avoid trivial objects. A circle is regarded as a graph without vertices as in [9].

The *genus* of a handlebody link is the sum of the genera of its components; a spatial graph is *trivalent* if the underlying graph is trivalent (each node has degree 3). By a slight abuse of notation, we also use HL (resp.  $G$ ) to denote the image of the embedding in  $\mathbb{S}^3$ . Let  $r$ HL (resp.  $rG$ ) be the mirror image of HL (resp.  $G$ ).

**Definition 2.2 (Equivalence).** *Two handlebody links HL, HL' (resp. spatial graphs  $G, G'$ ) are equivalent if they are ambient isotopic; they are equivalent up to mirror image if HL (resp.  $G$ ) is equivalent to HL' or  $r$ HL' (resp.  $G'$  or  $rG'$ ).*

A regular neighborhood of a spatial graph defines a handlebody link, up to equivalence [22, 3.24], and a spine of a handlebody link HL is a spatial graph  $G$  with HL a regular neighborhood of  $G$  [9]. In practice, it is more convenient to consider spines that are trivalent.

**Lemma 2.1.** *Every handlebody link admits a (trivalent) spine.*

*Proof.* It suffices to prove the connected case. We suppose HK is a handlebody knot of genus  $g$ , and  $\mathbf{D} = \{D_1, \dots, D_{3g-3}\}$  is a set of disjoint incompressible disks in HK such that the complement  $\text{HK} \setminus \bigcup_i N(D_i)$  of their tubular neighborhoods  $N(D_i)$  in HK consists of  $2(g-1)$  3-balls, each of which has non-trivial intersection with exactly three components of  $\prod_{i=1}^{3g-3} \partial N(D_i)$ . Such a disk system always exists.

Let disks  $D_{i1}, D_{i2}, D_{i3}$  be components of  $B_i \cap (\bigcup_{k=1}^{3g-3} N(D_k))$ , and choose points  $v_{i1}, v_{i2}, v_{i3}$  in the interior of  $D_{i1}, D_{i2}, D_{i3}$  and a point  $v_i$  in the interior of  $B_i$ . Then, join  $v_i$  to  $v_{ij}$  by a path for each  $j$ ; this gives us a trivalent vertex. Repeat the construction for every  $i$ , and then glue the  $v_{ij}$  together so that the vertices  $v_{ij}$  and  $v_{i'j'}$  are identified if they are in the same  $N(D_k)$ , for some  $k$ . This way, we obtain a connected trivalent spine of HK with  $2(g-1)$  trivalent vertices.  $\square$

In general, a trivalent spine of a  $n$ -component handlebody link of genus  $g$  has  $2(g-n) = 2t$  trivalent vertices, and we call such a handlebody link a  $(n, t)$ -handlebody link. This paper is primarily concerned with the case  $t = 1$ .

**2.2. Diagrams.** Let  $\mathbb{S}^k = \mathbb{R}^k \cup \infty$ , and without loss of generality, it may be assumed handlebody links or spatial graphs are away from  $\infty$ .

**Definition 2.3 (Regular projection).** *A regular projection of a spatial graph  $G$  is a projection  $\pi : \mathbb{S}^3 \setminus \infty \rightarrow \mathbb{S}^2 \setminus \infty$  such that the set  $\pi^{-1}(x) \cap G$  is finite with its cardinality  $\#(\pi^{-1}(x) \cap G) \leq 2$  for any  $x \in \mathbb{S}^2 \setminus \infty$ , and no 0-simplex of the polygonal subset  $G$  of  $\mathbb{S}^3$  is in the preimage of a double point, a double point being a point  $x \in \mathbb{S}^2 \setminus \infty$  with  $\#(\pi^{-1}(x) \cap G) = 2$ .*

As with the case of knots, up to ambient isotopy, every spatial graph admits a regular projection: the idea is to choose a vector  $v$  neither parallel to a 1-simplex in the polygonal subset  $G \subset \mathbb{S}^3 \setminus \infty = \mathbb{R}^3$  nor in a plane containing a 0-simplex and a 1-simplex or two 1-simplices; then isotopy  $G$  slightly to remove those points  $x$  with  $\#\pi_v^{-1}(x) \cap G > 2$ , where  $\pi_v$  is the projection onto the plane normal to  $v$ .

**Definition 2.4 (Diagram of a spatial graph).** *A diagram of a spatial graph  $G$  is the image of a regular projection of  $G$  with relative height information added to each double point.*

The convention is to make breaks in the line corresponding to the strand passing underneath; thus each double point becomes a *crossing* of the diagram.

**Definition 2.5 (Diagram of a handlebody link).** *A diagram of a handlebody link HL is a diagram of a spine of HL.*

A diagram of  $G$  (resp. HL) is trivalent if it is obtained from a regular projection of a trivalent spatial graph (resp. spine).

**Definition 2.6 (Crossing numbers).** *The crossing number  $c(D)$  of a diagram  $D$  of a handlebody link HL (resp. of a spatial graph  $G$ ) is the number of crossings in  $D$ . The crossing number  $c(\text{HL})$  of HL (resp.  $c(G)$  of  $G$ ) is the minimum of the set*

$$\{c(D) \mid D \text{ a diagram of HL (resp. } G)\}.$$

**Definition 2.7 (Minimal diagram).** *A minimal diagram  $D$  of a handlebody link HL (resp. of a spatial graph  $G$ ) is a diagram of HL (resp.  $G$ ) with  $c(D) = c(\text{HL})$  (resp.  $c(D) = c(G)$ ).*

Every multi-valent vertex in a minimal diagram  $D$  can be replaced with some trivalent vertices by the inverse of the contraction move [9, Fig. 1] without changing the crossing number, so for a handlebody link (resp. a spatial graph) there always exists a trivalent minimal diagram  $D$ . From now on, we shall use the term “a diagram” to refer to a trivalent diagram of either a spatial graph or a handlebody link.

Observe that, regarding each crossing as a quadrivalent vertex, we obtain a plane graph, a finite graph embedded in the 2-sphere. In practice, we work backward and start with a plane graph having only trivalent and quadrivalent vertices, and produce diagrams by replacing quadrivalent vertices with under- or over-crossings. If the plane graph has  $2t$  trivalent vertices and  $c$  quadrivalent vertices, then we can recover  $2^{c-1}$  diagrams from it, up to mirror image. In particular, a  $c$ -crossing  $(n, t)$ -handlebody link can be recovered from one of these plane graphs. Therefore if one can enumerate all plane graphs with  $2t$  trivalent vertices and up to  $c$  quadrivalent vertices, then one can find all  $(n, t)$ -handlebody links up to  $c$  crossings.

**2.3. Moves.**

**Definition 2.8 (Moves).** *Local changes in a diagram depicted in Fig. 2.1 and Fig. 2.2 are called generalized Reidemeister moves, and the local change in Fig. 2.3 is called an IH-move.*

Note that spines of equivalent handlebody links might be inequivalent as spatial graphs; indeed, the following holds.

**Theorem 2.2** ([12, Theorem 2.1], [26]). *Two trivalent spatial graphs are equivalent if and only if their diagrams are related by a finite sequence of generalized Reidemeister moves.*

**Theorem 2.3** ([9, Corollary 2]). *Two handlebody links are equivalent if and only if their trivalent diagrams are related by a finite sequence of generalized Reidemeister moves and IH-moves.*

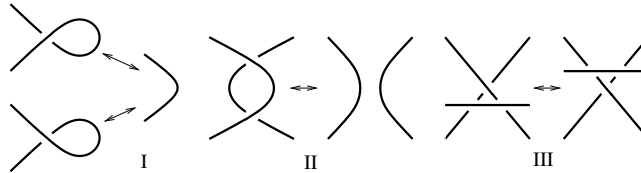


FIGURE 2.1. Classical Reidemeister moves of type I, II, III.

When analyzing the data from the code (Appendix A), it is more convenient to call a diagram IH-minimal if the number of crossings cannot be reduced by generalized Reidemeister moves and IH moves, that is, “minimal” as a diagram of a *handlebody link*, and to call a diagram R-minimal if the number of crossings cannot be reduced by generalized Reidemeister moves, that is, “minimal” as a diagram of a *spatial graph*.

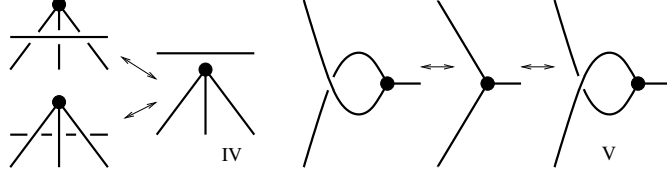


FIGURE 2.2. Reidemeister moves IV and V involve a triple point.

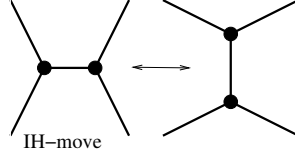


FIGURE 2.3. The IH-move.

#### 2.4. Non-split, irreducible handlebody links.

**Definition 2.9 (Edge connectivity of a graph).** *The edge-connectivity of a graph is the minimum number of edges whose deletion disconnects the graph.*

**Definition 2.10 (Connectivity of a diagram).** *A diagram has  $e$ -connectivity if its underlying plane graph has edge-connectivity  $e$ .*

**Definition 2.11 (Split handlebody link).** *A handlebody link HL is split if there exists a 2-sphere  $\mathfrak{S} \subset \mathbb{S}^3$  such that  $\mathfrak{S} \cap \text{HL} = \emptyset$  and both components of the complement  $\mathbb{S}^3 \setminus \mathfrak{S}$  have non-trivial intersection with HL.*

**Definition 2.12 (Reducible handlebody link).** *A handlebody link HL is reducible if its complement admits a 2-sphere  $\mathfrak{S}$  such that  $\mathfrak{S} \cap \text{HL}$  is an incompressible disk in HL; otherwise it is irreducible.*

Note that  $\mathfrak{S}$  in Definition 2.12 factorizes HL into two handlebody links, each called a *factor* of the factorization of HL.

A diagram with 0-connectivity (resp. 1-connectivity) represents a split (resp. reducible) handlebody link, so only diagrams with connectivity greater than 1 are of interest to us; on the other hand, the connectivity of a diagram of a  $(n, t)$ -handlebody link with  $t > 0$  cannot exceed 3.

Now, we recall the order-2 vertex connected sum between spatial graphs [17], which is used to produce handlebody links represented by minimal diagrams with 2-connectivity. A trivial ball-arc pair of a spatial graph  $G$  is a 3-ball  $B$  with  $G \cap B$  a trivial tangle in  $B$ ; it is oriented if an orientation of  $G \cap B$  is given.

**Definition 2.13 (Knot sum).** *Given two spatial graphs  $G_1, G_2$  with oriented trivial ball-arc pairs  $B_1, B_2$  of  $G_1, G_2$ , respectively, their order-2 vertex connected sum  $(G_1, B_1) \# (G_2, B_2)$  is a spatial graph obtained by removing the interiors of  $B_1, B_2$  and gluing the resulting manifolds  $\overline{\mathbb{S}^3 \setminus B_1}$  and  $\overline{\mathbb{S}^3 \setminus B_2}$  by an orientation-reserving homeomorphism*

$$h : (\partial(\overline{\mathbb{S}^3 \setminus B_1}), \partial(G_1 \cap B_1)) \rightarrow (\partial(\overline{\mathbb{S}^3 \setminus B_2}), \partial(G_2 \cap B_2)).$$

The notation  $G_1 \# G_2$  denotes the set of order-2 vertex connected sums of  $G_1, G_2$  given by all possible trivial ball-arc pairs.

Since an order-2 vertex connected sum depends only on the edges of  $G_1, G_2$  intersecting with  $B_1, B_2$  and their orientations,  $G_1 \# G_2$  is a finite set.

3. UNIQUENESS, NON-SPLITABILITY, AND IRREDUCIBILITY

Recall that, given a finite group  $G$ , the Kitano-Suzuki invariant  $ks_G(\text{HL})$  of a handlebody link  $\text{HL}$  is the number of conjugate classes of homomorphisms from  $\pi_1(\overline{\mathbb{S}^3 \setminus \text{HL}})$  to  $G$  [13]. Table 2 lists the invariants  $ks_{A_4}(\text{HL})$  and  $ks_{A_5}(\text{HL})$  of each handlebody link  $\text{HL}$  in Table 1,  $A_k$  being the alternating group on  $k$  letters, as well as an upper bound of the rank of  $\pi_1(\overline{\mathbb{S}^3 \setminus \text{HL}})$  computed by Appcontour [21].

The entry “split” refers to the split handlebody link  $\text{HL}$  given by a trivial handlebody knot and an unknotted solid torus; the entry “fake  $6_5$ ” is the split handlebody link consisting of the handlebody knot  $\text{HK } 4_1$ , Ishii-Kishimoto-Suzuki-Moriuchi’s  $4_1$  in [10], and an unknotted solid torus; the entry “fake  $6_{11}$ ” is  $6_{11}$  in Table 1 with one of the bottom crossings reversed, thus making the lower solid torus component split off.

TABLE 2. Kitano-Suzuki invariant for entries in Table 1.

handlebody link	components	$ks_{A_4}$	$ks_{A_5}$	rank
split	trivial + unknot	178	3675	3
$4_1$	trivial + unknot	114	600	3
$5_1$	trivial + unknot	98	660	$\leq 4$
$6_1$	trivial + unknot	90	600	3
$6_2$	trivial + unknot	106	689	3
$6_3$	trivial + unknot	90	469	3
$6_4$	$\text{HK}4_1$ + unknot	106	689	3
$6_5$	$\text{HK}4_1$ + unknot	210		$\leq 4$
fake $6_5$	$\text{HK}4_1$ + unknot	274		
$6_6$	trivial + unknot	130	1380	3
$6_7$	trivial + unknot	98	597	$\leq 4$
$6_8$	trivial + unknot	114	1401	3
$6_9$	trivial + 2 unknots	310	1841	4
$6_{10}$	trivial + 2 unknots	326		4
$6_{11}$	trivial + 2 unknots	486	5876	4
fake $6_{11}$	trivial + 2 unknots	694		
$6_{12}$	trivial + 2 unknots	502	5883	4
$6_{13}$	trivial + 2 unknots	822		4
$6_{14}$	trivial + 2 unknots	486	5876	4
$6_{15}$	trivial + 3 unknots	1242		5

**Theorem 3.1 (Uniqueness).** *Entries in Table 1 are all inequivalent.*

*Proof.* All entries in Table 1 except for the pairs  $(6_2, 6_4)$  and  $(6_{11}, 6_{14})$  are distinguished by comparing their  $ks_{A_4}$  and  $ks_{A_5}$  invariants (shown in Table 2). On the other hand,  $6_2$  and  $6_4$  cannot be equivalent because the removal of the “unknot” component produces inequivalent handlebody knots: one being trivial, the other being  $\text{HK } 4_1$ . Similarly, one can distinguish  $6_{11}$  and  $6_{14}$  by removing the solid torus component having a non-trivial linking number with the genus 2 handlebody component [16] in each of them, and observing that, for  $6_{14}$ , the resulting handlebody link is  $4_1$ , whereas for  $6_{11}$ , we get the trivial split handlebody link.  $\square$

*Remark 3.1.* The pairs  $(6_2, 6_4)$  and  $(6_{11}, 6_{14})$  in fact have homeomorphic complements, and hence the fundamental group cannot discriminate. Fig. 3.1 and 3.2 illustrate how to obtain the complements of  $6_2$  and  $6_{11}$  from  $6_4$  and  $6_{14}$ , respectively, via 3-dimensional Dehn-twists (indicated by arrows).

*Remark 3.2.*  $6_5$  viewed as a diagram of a spatial graph is the notorious figure eight puzzle devised by Steward Coffin [3]. The goal of the puzzle is to free the circle component from the knotted handcuff graph, i.e. to obtain the fake  $6_5$  as a spatial graph. The impossibility of solving the puzzle then follows from computing  $ks_{A_4}(\bullet)$  of  $6_5$  and fake  $6_5$  (Table 2). See [1], [15] for other proofs of this.

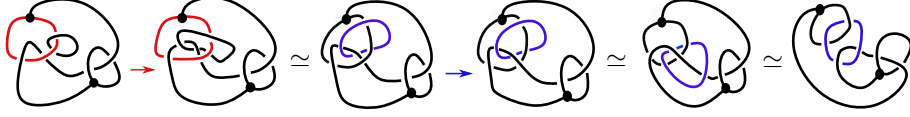


FIGURE 3.1.  $6_2$  and  $6_4$  have homeomorphic complements.



FIGURE 3.2.  $6_{11}$  and  $6_{14}$  have homeomorphic complements.

**Theorem 3.2 (Unsplittability).** *Entries in Table 1 are all unsplittable.*

*Proof.* In most cases ( $5_1, 6_1, 6_2, 6_3, 6_4, 6_7, 6_9, 6_{10}$ ) unsplittability follows by computing the linking number [16] between pairs of components of a handlebody link. There are a few cases where the linking number vanishes, and we deal with these cases by computing the  $ks_{A_4}$ - and  $ks_{A_5}$ -invariants of the corresponding split handlebody links (Table 2).

If  $6_5$  were split, then  $6_5$  would be equivalent to the fake  $6_5$  but this is not possible by Table 2. In the case of  $4_1, 6_6, 6_8$ , if any of them were split, than it would be equivalent to “split” in Table 2, but that is not the case. A similar argument can be applied to  $6_{11}$  and  $6_{14}$ : if one of them were split, it would be equivalent to the fake  $6_{11}$ , in contradiction to Table 2. Lastly, we observe that  $6_{12}$  and  $6_{13}$  are non-split, for otherwise  $4_1$  would be split.  $\square$

Below we recall the irreducibility test developed in [2]. A  $r$ -generator link is a link whose knot group, the fundamental group of its complement, is of rank  $r$ .

**Lemma 3.3.** *If the trivial knot is a factor of some factorization of a reducible  $(n, 1)$ -handlebody link HL, then*

$$12 \mid ks_{A_4}(\text{HL}) + 6 \cdot 3^n + 2 \cdot 4^n \quad \text{and} \quad 60 \mid ks_{A_5}(\text{HL}) + 14 \cdot 4^n + 19 \cdot 3^n + 22 \cdot 5^n. \quad (3.1)$$

**Lemma 3.4.** *If a 2-generator knot is factor of some factorization of a reducible  $(n, 1)$ -handlebody link HL, then*

$$12 + 24p \mid ks_{A_4}(\text{HL}) + (6 + 16p) \cdot 3^n + (2 + 6p) \cdot 4^n, \quad \text{where } p = 0 \text{ or } 1. \quad (3.2)$$

**Lemma 3.5.** *If a 2-component, 2-generator link is a factor of some factorization of a reducible  $(n, 1)$ -handlebody link HL, then*

$$48 + 24p \mid ks_{A_4}(\text{HL}) + (26 + 16p) \cdot 3^{n-1} + (8 + 6p) \cdot 4^{n-1}, \quad \text{where } p = 0, 1, 2, 3 \text{ or } 4. \quad (3.3)$$

From the above lemmas, one derives the following irreducibility test (see [2] for more details), making use of the Grushko theorem [6].



**Corollary 3.6 (Irreducibility test).** *A 3-generator  $(2, 1)$ -handlebody link is irreducible if it fails to satisfy (3.1); a 4-generator  $(2, 1)$ -handlebody link is irreducible if it fails to satisfy (3.2); a 4-generator  $(3, 1)$ -handlebody link or a 5-generator  $(4, 1)$ -handlebody link is irreducible if it fails to satisfy (3.1) and (3.3).*

**Theorem 3.7 (Irreducibility).** *Entries in Table 1 are irreducible.*

*Proof.* Corollary 3.6, together with Table 2, shows that all but  $6_9, 6_{12}$  are irreducible. The irreducibility of  $6_{12}$  and  $6_9$  follows from computing the linking number between each pair of components in each of them. Specifically, if  $6_{12}$  (resp.  $6_9$ ) is reducible, then either the trivial knot or a 2-generator 2-component link is a factor of some factorization of  $6_{12}$  (resp.  $6_9$ ). For  $6_{12}$ , the former case is not possible by (3.1); the latter impossible too, for otherwise the two solid torus components would have a trivial linking number. The same argument implies that  $6_9$  cannot have a 2-generator 2-component link as a factor, and the trivial knot cannot be its factor either, since the homomorphism of integral homology

$$H_1(V_1) \oplus H_1(V_2) \rightarrow H_1(\overline{\mathbb{S}^3 \setminus W})$$

is onto, where  $V_1, V_2$  are the solid torus components, and  $W$  the genus 2 component. □

*Remark 3.3.* The complement of  $6_9$  is in fact  $\partial$ -reducible; one can see this by performing the twist operation, indicated by the arrow in Fig. 3.3, where it shows that its complement is homeomorphic to the complement of the order-1 connected sum (Definition 6.1) between two Hopf links (Fig. 3.3, right). In the connected case, no irreducible handlebody knot of genus 2 admits a  $\partial$ -reducible complement [24, Theorem 1], but when the genus is larger than 2, such handlebody knots exist [23, Example 5.5], [24, Section 5]. For a  $(n, 1)$ -handlebody link, we suspect that  $6_9$  attains the lowest possible  $n$  for such a phenomenon to happen.

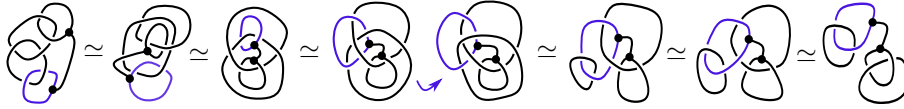


FIGURE 3.3.  $6_9$  and fake  $6_9$ .

#### 4. COMPLETENESS

This section discusses completeness of Table 1. Recall first that a minimal diagram of a non-split, irreducible handlebody link has either 2- or 3-connectivity. IH-minimal diagrams with 3-connectivity are obtained from a software code, and IH-minimal diagrams with 2-connectivity are recovered by knot sum of spatial graphs.

**4.1. Minimal diagrams with 3-connectivity.** We consider plane graphs with two trivalent vertices and up to six quadrivalent vertices satisfying the properties:

- (1) each of them has edge-connectivity 3 as an abstract graph,
- (2) their double arcs can only connect two quadrivalent vertices as abstract graphs, and
- (3) their double arcs only form a “bigon” (a polygon with two sides; the case ‘i’ in Fig. 4.1) as plane graphs.

The reason of considering only double arcs connecting two quadrivalent vertices with a bigon configuration is because all the other cases lead to either non-R-minimal diagrams or diagrams with connectivity less than 3 (see Fig. 4.1, where

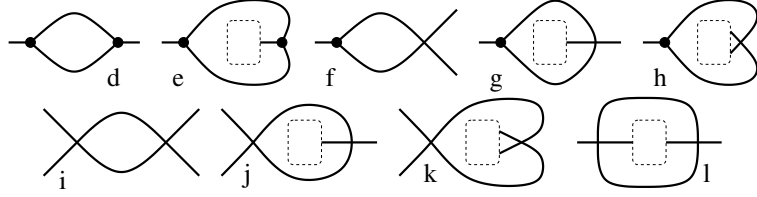


FIGURE 4.1. Possible configurations for loops and double arcs.

“d, e, f, g, h” illustrate those double arcs connecting at least one trivalent vertex and “j, k, l” those connecting two quadrivalent vertices with a non-bigon configuration.)

We enumerate such plane graphs by the software code, and then recover diagrams from these plane graphs by adding an over- or under-crossing to each quadrivalent vertex. Note that the number ( $n$  in Table 3) of components of the associated spatial graphs is independent of how over/under-crossings are chosen. To provide a glimpse of how the code works, we record in Table 3 the number of such plane graphs with  $c$  quadrivalent vertices for each  $n$ . To recover  $(n, 1)$ -handlebody links with  $n > 1$  represented by IH-minimal diagrams with 3-connectivity, we need to consider the cases with  $n > 1$  in Table 3. On the other hand, to produce  $(n, 1)$ -handlebody links represented by IH-minimal diagrams with 2-connectivity, spatial graphs admitting an R-minimal diagram with 3-connectivity up to 4 crossings are required; thus all cases with  $c \leq 4$  have to be examined.

TABLE 3. Plane graphs given by the code.

$c$	$n = 1$	$n = 2$	$n = 3$	<b>total</b>
2	1			1
3	2	1		3
4	8	2		10
5	29	8		37
6	144	34	3	181

**IH-minimal diagrams.** We examine IH-minimality of diagrams produced by plane graphs with  $n \geq 2$ , and discard those obviously not IH-minimal. This excludes all diagrams produced by the code up to 5 crossings (Table 7), but for diagrams with 6 crossings, some diagrams are potentially IH-minimal: they represent handlebody links  $6_1, 6_2, 6_3$  or  $6_9$  in Table 1.

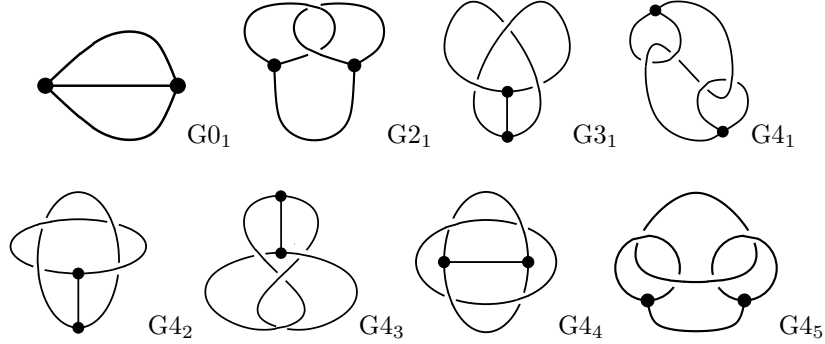
**Lemma 4.1.** *An IH-minimal diagram with 3-connectivity has crossing number  $c \geq 6$ , and if  $c = 6$ , it represents a handlebody link equivalent to  $6_1, 6_2, 6_3$  or  $6_9$ , up to mirror image.*

Note that we cannot conclude diagrams of  $6_1, 6_2, 6_3$  and  $6_9$  in Table 1 are IH-minimal yet, as they might admit diagrams with 2-connectivity and fewer crossings.

**R-minimal diagrams.** To produce minimal diagrams with 2-connectivity up to 6 crossings, we need R-minimal diagrams up to 4 crossings. Inspecting R-minimality of diagrams produced by the code (Table 6) gives us the following lemma.

**Lemma 4.2.** *An R-minimal diagram with 3-connectivity and crossing number less than 5 represents one of the spatial graphs in Table 4, up to mirror image.*

TABLE 4. Spatial graphs up to four crossings.



**4.2. Minimal diagrams with 2-connectivity.** Recall a diagram  $D$  with 2-connectivity can be decomposed into finitely many simpler tangle diagrams such that each associated diagram of spatial graphs has 3- or 4-connectivity (Fig. 1.1). Furthermore, if  $D$  is  $R$ -minimal, each induced spatial graph diagram is also  $R$ -minimal. In particular, an  $IH$ -minimal diagram with 2-connectivity can be recovered by performing the order-2 vertex connected sum between spatial graphs admitting a minimal diagram with  $k$ -connectivity,  $k > 2$ . Since we are interested in  $(n, 1)$ -handlebody links, only one summand is a spatial graph with two trivalent vertices, and the rest are links admitting a minimal diagram with 4-connectivity. Note that the simplest minimal diagram with 4-connectivity represents the Hopf link, and since we only consider minimal diagrams up to 6 crossings, there are at most three link summands. Thus,  $IH$ -minimal diagrams with 2-connectivity can be recovered by considering the seven possible configurations below:

- (1)  $G\#L_1$ ,
- (2)  $(G\#L_1)\#L_2$ ,
- (3)  $G\#(L_1\#L_2)$ ,
- (4)  $((G\#L_1)\#L_2)\#L_3$ ,
- (5)  $(G\#L_1)\#(L_2\#L_3)$ ,
- (6)  $(G\#(L_1\#L_2))\#L_3$ ,
- (7)  $G\#((L_1\#L_2)\#L_3)$ ,

where  $G$  is a spatial graph admitting a minimal diagram with 3-connectivity, and  $L_i$  is a link admitting a minimal diagram with 4-connectivity. In general it is not known if a minimal diagram with 4-connectivity always represents a prime link; it is the case, however, when the crossing number is less than 5. In fact, there are only four minimal diagrams with 4-connectivity up to 4 crossings, and they represent the Hopf link, the trefoil knot, the figure eight, and Solomon’s knot (L4a1), respectively.

**Cases 4 through 7** are easily dealt with since  $G$  must have no crossings, and hence it is the trivial theta curve  $G_{0_1}$ , and thus each  $L_i$  is necessarily the Hopf link, so the knot sums actually consist in ‘inserting a ring’ somewhere to the result of the previous knot sums. To produce irreducible handlebody links there is only one possibility, that is, adding one Hopf link to each of the three arcs of the trivial theta curve, and this gives us entry  $6_{15}$  in Table 1.

**Cases 2 and 3** forces  $G$  to have 2 crossings at most. It cannot have zero crossings (trivial theta curve), for otherwise, we could only get diagrams representing reducible handlebody links. Note also that there is no  $R$ -minimal diagram with 1 crossing. Now, there is only one  $R$ -minimal diagram with two crossings, this is, entry  $G_{2_1}$  in Table 4 (Moriuchi’s  $2_1$  in [18]).

Now, to add two Hopf links to it, i.e. to place two rings successively, we observe that one of them must be placed around the connecting arc of the handcuff graph

by irreducibility. The second ring can be placed in three inequivalent ways, which yield entries  $6_{12}$ ,  $6_{13}$  and  $6_{14}$  of Table 1.

**Case 1** is more complicated, and we divided it into subcases based on the crossing number  $c := c(G)$ . The case  $c = 0$  is immediately excluded by irreducibility, so three possibilities remain:  $c \in \{2, 3, 4\}$ .

*Subcase  $c(G) = 2$ .*  $G$  is necessarily  $G2_1$  in Table 4, and  $L$  cannot be a knot. Since the crossing number of  $L$  cannot exceed 4,  $L$  is either L2a1 (Hopf link) or L4a1 (Solomon's knot). In either case,  $L$  is to be added to the connecting arc of the handcuff graph to produce irreducible handlebody links, yielding entries  $4_1$  and  $6_8$  in Table 1.

*Subcase  $c(G) = 3$ .*  $G$  is necessarily  $G3_1$  (Moriuchi's theta curve  $3_1$  in [17]), so  $L$  cannot be a knot, and hence is the Hopf link. There is only one place to add  $L$  by irreducibility, and this leads to entry  $5_1$  in Table 1.

*Subcase  $c(G) = 4$ .* In this case,  $L$  can only be the Hopf link; and there are five possible spatial graphs for  $G$ , namely  $G4_1$ ,  $G4_2$ ,  $G4_3$ ,  $G4_4$ , and  $G4_5$ :

- For  $G4_1$  in Table 4 (Moriuchi's non-prime handcuff graph  $2_1\#_3 2_1$  [19]), there are two inequivalent ways to add  $L$  which produce entries  $6_4$  and  $6_5$ .
- For  $G4_2$  and  $G4_3$  in Table 4 (Moriuchi's prime handcuff graph  $4_1$  [18] and prime theta-curve  $4_1$  [17], respectively), there is only one way to add the Hopf link in each case by irreducibility, and this gives  $6_6$ ,  $6_7$  in Table 1, respectively.
- For  $G4_4$  and  $G4_5$  in Table 4, again by irreducibility, there is only one way to add the Hopf link in each case, which gives us  $6_{10}$  and  $6_{11}$  in Table 1, respectively.

We summarize the discussion above in the following:

**Lemma 4.3.** *A non-split, irreducible handlebody link admitting an IH-minimal diagram with 2-connectivity and crossing number  $\leq 6$  is equivalent, up to mirror image, to one of the following handlebody links:*

$$4_1, 5_2, 6_4, 6_5, 6_6, 6_7, 6_8, 6_{10}, 6_{11}, 6_{12}, 6_{13}, 6_{14}. \quad (4.1)$$

By Lemma 4.1, if any of (4.1) admits an IH-minimal diagram with 3-connectivity, it is equivalent to one of  $6_1, 6_2, 6_3, 6_9$ , while by Lemma 4.1 if  $6_1, 6_2, 6_3$  or  $6_9$  admits an IH-minimal diagram with 2-connectivity and less than 6 crossings, it is equivalent to  $4_1$  or  $5_1$ , but neither situation can happen by Theorem 3.1.

**Corollary 4.4.** *Diagrams in Table 1 are all IH-minimal.*

## 5. CHIRALITY

**5.1. Decomposable links.** We consider order-2 connected sum (compare with Definition 6.1) for handlebody-link-disk pairs. A handlebody-link-disk pair is a handlebody link HL with an oriented incompressible disk  $D \subset \text{HL}$ . A trivial knot with a meridian disk is considered as the trivial handlebody-link-disk pair.

**Definition 5.1 (Order-2 connected sum).** *Given two handlebody-link-disk pairs  $(\text{HL}_1, D_1)$ ,  $(\text{HL}_2, D_2)$  the order-2 connected sum  $(\text{HL}_1, D_1)\#(\text{HL}_2, D_2)$  is obtained as follows: first choose a 3-ball  $B_i$  of  $D_i$  in  $\mathbb{S}^3$  for each  $i$  with  $\overline{B_i} \cap \text{HL}_i$  a tubular neighborhood  $N(D_i)$  of  $D_i$  in  $\text{HL}_i$ ; next, identify  $\overline{N(D_i)}$  with  $D_i \times [0, 1]$  via the orientation of  $D_i$ . Then  $(\text{HL}_1, D_1)\#(\text{HL}_2, D_2)$  is given by removing  $\overline{B_i}$  and gluing the resulting manifolds via an orientation-reversing homeomorphism:*

$$h : \partial(\overline{\mathbb{S}^3 \setminus B_1}) \rightarrow \partial(\overline{\mathbb{S}^3 \setminus B_2}) \quad \text{with } h(D_1 \times \{j\}) = D_2 \times \{k\}, \quad k \equiv j + 1 \pmod{2}.$$

*A non-split, irreducible handlebody link is decomposable if it is equivalent to an order-2 connected sum of non-trivial handlebody-link-disk pairs.*

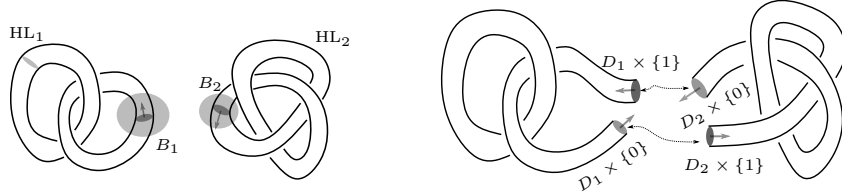


FIGURE 5.1. Knot sum of handlebody-link-disk pairs

Decomposability is reflected in minimal diagrams in most examples here, thus we state the following conjecture.

**Conjecture 5.1.** *Minimal diagrams of a decomposable handlebody link have 2-connectivity.*

**Lemma 5.2.** *For a non-split, irreducible handlebody link HL, the following statements are equivalent:*

- HL is decomposable;
- there exists a 2-sphere  $\mathfrak{S}$  in  $\mathbb{S}^3$  such that  $\mathfrak{S}$  and HL intersect at two incompressible disks in HL and neither of  $\overline{B_i \setminus \text{HL}}$ ,  $i = 1, 2$ , is a solid torus, where  $B_1, B_2$  are components of  $\overline{\mathbb{S}^3 \setminus \mathfrak{S}}$ ;
- $\overline{\mathbb{S}^3 \setminus \text{HL}}$  admits an incompressible, non-boundary parallel (or  $\partial$ -incompressible) annulus  $A$  with  $\partial A$  inessential in HL.

*Proof.* This follows from the definition of ( $\partial$ -) incompressibility. □

The annulus  $A$  in Lemma 5.2 is called a decomposing annulus of HL. Similarly, a decomposing annulus  $A$  of a handlebody-link-disk pair  $(\text{HL}, D)$  is an incompressible, non-boundary parallel annulus  $A$  with  $\partial A$  inessential in HL and disjoint from  $\partial D$ ; note that HL in  $(\text{HL}, D)$  could be reducible.

We now prove a unique decomposition theorem for handlebody links with no genus  $g > 2$  component; a unique decomposition theorem for handlebody knots of arbitrary genus is given [14, Appendix B] (see also [11]).

**Theorem 5.3.** *Given a non-split, irreducible handlebody link HL, suppose no component of HL has genus greater than 2, and  $A, A'$  are decomposing annuli inducing*

$$\text{HL} \simeq (\text{HL}_1, D_1) \# (\text{HL}_2, D_2), \text{HL} \simeq (\text{HL}'_1, D'_1) \# (\text{HL}'_2, D'_2), \text{ respectively.} \quad (5.1)$$

*If  $(\overline{\mathbb{S}^3 \setminus \text{HL}_i}, D_i), i = 1, 2$ , admits no decomposing annulus. Then  $A, A'$  are isotopic, in the sense that there exists an ambient isotopy  $f_t : \mathbb{S}^3 \rightarrow \mathbb{S}^3$  fixing HL with  $f_1(A) = A'$ .*

*Proof.* Note first that if  $A, A'$  are disjoint, then the assumption implies that they must be parallel and hence isotopic. Suppose  $A \cap A' \neq \emptyset$ . Then we isotopy  $A$  such that the number of components of  $A \cap A'$  is minimized.

**Claim: any circle or arc in  $A \cap A'$  is essential in both  $A$  and  $A'$ .** Observe first that a circle component  $C$  of  $A \cap A'$  is either essential or inessential in both  $A$  and  $A'$ , for assuming otherwise would contradict the incompressibility of  $A, A'$ . Suppose  $C$  is inessential in both  $A$  and  $A'$ , and is innermost in  $A'$ . Then  $C$  bounds disks  $D, D'$  in  $A, A'$ , respectively. Since HL is non-split,  $D \cup D'$  bounds a 3-ball  $B$  in  $\overline{\mathbb{S}^3 \setminus \text{HL}}$ . Isotopy  $D$  across  $B$  to  $D'$  induces a new annulus  $A$  isotopic to the original one with  $A \cap A'$  having less components, contradicting the minimality.

Similarly, if  $l$  is an arc component of  $A \cap A'$ , then it is either essential or inessential in both  $A$  and  $A'$ , for assuming otherwise would contradict the  $\partial$ -incompressibility of  $A, A'$ . Suppose  $l$  is inessential in both  $A$  and  $A'$  and an innermost arc in  $A'$ .

Then  $l$  cuts off a disk  $D'$  from  $A'$  and a disk  $D$  from  $A$ . Let  $\hat{D} := D \cup D'$ . If  $\partial\hat{D}$  is inessential, then we can remove the intersection  $l$  by isotopying  $A$  across the ball bounded by  $\hat{D}$  and the disk bounded by  $\partial\hat{D}$  in  $\partial\text{HL}$ , contradicting the minimality. If  $\partial\hat{D}$  is essential, then isotopying  $\hat{D}$ , we can disjoint  $\hat{D}$  from  $A$ .

Now, it may be assumed that  $D_1$  is in a genus one component of  $\text{HL}_1$ , and hence  $D_2$  is in a component of  $\text{HL}_2$  with genus  $\leq 2$ . Since  $\partial\hat{D}$  is essential,  $\hat{D}$  has to be in a genus 2 component of  $\text{HL}_2$  containing  $D_2$ . Because  $\partial\hat{D} \cap D_2 = \emptyset$ , if  $\partial\hat{D}$  is essential on the boundary of the embedded solid torus  $(\text{HL}_2 \setminus N(D_2)) \subset \mathbb{S}^3$ ,  $\partial\hat{D}$  would be its longitude, where  $N(D_2)$  is a tubular neighborhood of  $D_2$ , disjoint from  $\hat{D}$ , in  $\text{HL}_2$ . Particularly,  $\text{HL}_2$  and therefore  $\text{HL}$  would be reducible, a contradiction. On the other hand, if  $\partial\hat{D}$  bounds a disk on  $\partial(\text{HL}_2 \setminus N(D_2))$  that contains some components of  $\partial\overline{N(D_2)}$ , then  $\partial\hat{D}$  is inessential in  $\text{HL}_2$ , and hence in  $\text{HL}$ , again contradicting the irreducibility of  $\text{HL}$ .

The claim is proved, which also implies  $A \cap A'$  contains either circles or arcs.

**No essential circles.** Suppose  $C$  is an essential circle, and a closest circle to  $\partial A'$ . Let  $R'$  be the annulus cut off by  $C$  from  $A'$  with  $A \cap R' = C$  and  $R$  an annulus cut off by  $C$  from  $A$ . We isotopy the incompressible annulus  $\hat{R} := R \cup R'$  away from  $A$ . Since components of  $\partial\hat{R}$  are inessential in  $\text{HL}$ , by the assumption,  $\hat{R}$  is either parallel to  $A$  or boundary-parallel. In the former case, replacing  $A$  with  $R$  leads to a contradiction since  $R \cap A'$  has less components than  $A \cap A'$ . In the latter case, isotopying  $R$  through the solid torus  $V$  bounded by  $\hat{R}$  and the part of  $\partial\text{HL}$  parallel to  $\hat{R}$  gives a new  $A$  isotopic to the original one but with less components in  $A \cap A'$ , contradicting the minimality.

**No essential arcs.** Suppose  $l_1$  is an essential arc. Then choose the essential arc  $l_2$  next to  $l_1$  in  $A'$  such that the disk  $D'$  cut off by  $l_1, l_2$  from  $A'$  has  $D' \cap A = l_1 \cup l_2$  and is on the side of  $A$  containing components of  $\text{HL}_1$ . Let  $D$  be a disk cut off by  $l_1, l_2$  from  $A$ . It may be assumed, by pushing  $D$  away from  $A$ , that  $D \cup D'$  is disjoint from  $A$ , and hence is on the genus 1 complement of  $\text{HL}_1$  containing  $D_1$ . Since  $\hat{A} := D \cup D'$  is disjoint from  $D_1$ , it is necessarily an annulus, for if it were a Möbius band, we would get a non-orientable surface embedded in  $\mathbb{S}^3$ . Furthermore, each component of  $\partial\hat{A}$  is necessarily inessential in  $\text{HL}_1$ , so it either bounds a meridian disk or is inessential in  $\partial\text{HL}_1$ . Note also it cannot be the case that one component of  $\partial\hat{A}$  is essential in  $\partial\text{HL}_1$  and the other inessential by the irreducibility of  $\text{HL}$ . Suppose both components are inessential in  $\partial\text{HL}_1$ . Then  $\hat{A}$ , together with disks on  $\partial\text{HL}_1$  bounded by  $\partial\hat{A}$ , bounds a 3-ball, with which we can isotopy  $A$  to remove the intersection  $l_1, l_2$ , contradicting the minimality. Suppose both components bound meridian disks in  $\text{HL}_1$ . Then  $\tilde{A} = D^c \cup D'$  has  $\partial\tilde{A}$  inessential in  $\partial\text{HL}_1$ , where  $D^c = \overline{A \setminus D}$ . Thus we reduce it to the previous case.  $\square$

**5.2. Chirality.** We divide the proof of Theorem 1.2 into two lemmas.

**Lemma 5.4.** *All handlebody links except for  $5_1, 6_3, 6_6, 6_7, 6_8, 6_{10}$  in Table 1 are achiral.*

*Proof.* Except  $6_2$ , equivalences between these handlebody links and their mirror images are easy to construct; an equivalence between  $6_2$  and  $r6_2$  is depicted in Fig. 5.2  $\square$

**Lemma 5.5.**  *$5_1, 6_3, 6_6, 6_7, 6_8, 6_{10}$  in Table 1 are chiral.*

*Proof.* Recall that, given a handlebody link  $\text{HL}$ , if  $\text{HL}$  and  $r\text{HL}$  are equivalent, then there is an orientation-reversing self-homeomorphism of  $\mathbb{S}^3$  sending  $\text{HL}$  to  $\text{HL}$ .

Observe that each of  $5_1, 6_6, 6_8, 6_{10}$  admits an obvious decomposing annulus satisfying conditions in Theorem 5.3; particularly the annulus in each of them is unique. Their chirality then follows readily from the fact that torus links are chiral.



FIGURE 5.2.  $6_2$  and its mirror image.

To see chirality of  $6_3$ , we observe that, given a  $(2, 1)$ -handlebody link  $HL$ , any self-homeomorphism of  $\mathbb{S}^3$  preserving  $HL$  sends the meridian  $m$  and the preferred longitude  $l$  of the circle component to  $m^{\pm 1}$  and  $l^{\pm 1}$ , respectively. In particular, any isomorphism on knot groups induced by such a homeomorphism sends the conjugacy class of  $m \cdot l$  in  $\pi_1(\mathbb{S}^3 \setminus \overline{HL})$  to the conjugacy class of  $m \cdot l$ ,  $m^{-1} \cdot l$ ,  $m \cdot l^{-1}$  or  $m^{-1} \cdot l^{-1}$ , depending on whether the homeomorphism is orientation-preserving.

Let  $N$  be the number of conjugacy classes of homomorphisms from  $\pi_1(\mathbb{S}^3 \setminus \overline{HL})$  to a finite group  $G$  that sends  $m \cdot l$  (and hence  $m^{-1} \cdot l^{-1}$ ) to 1, and  $rN$  the number of conjugacy classes of homomorphisms from  $\pi_1(\mathbb{S}^3 \setminus \overline{HL})$  to  $G$  that sends  $m \cdot l^{-1}$  (and hence  $m^{-1} \cdot l$ ) to 1. Now, if  $HL$  and its mirror image  $rHL$  are equivalent, then  $N = rN$ . This is however not the case with  $6_3$ ; when  $G = A_5$ , we have  $(N, rN) = (77, 111)$  as computed by [21].

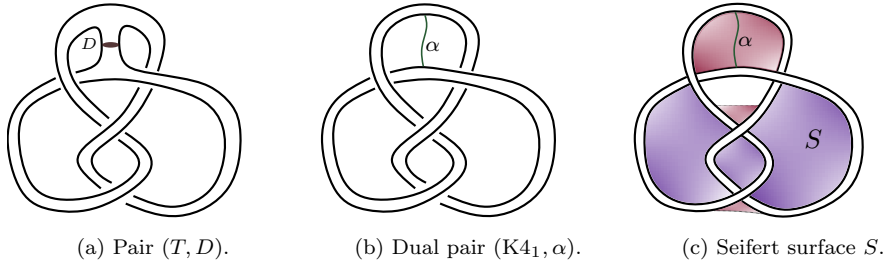


FIGURE 5.3.

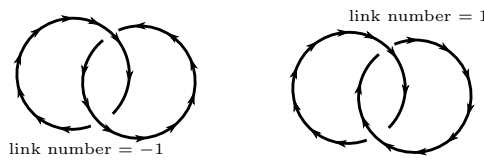


FIGURE 5.4. Hopf links with different orientations.

In the case of  $6_7$  by Theorem 5.3, every self-homeomorphism  $f$  of  $\mathbb{S}^3$  sending  $6_7$  to itself induces a self-homeomorphism  $f$  sending the handlebody-knot-disk pair  $(T, D)$  in Fig. 5.3a to itself, or alternatively the (fattened) figure eight with an arc  $(K4_1, \alpha)$  in Fig. 5.3b to itself, where  $\alpha$  is the dual one-simplex to  $D$ .

Let  $S$  be a minimal Seifert surface of the figure eight (Fig. 5.3c) containing the arc  $\alpha$ . Then it can be further assumed that  $f(S) = S$ , because the complement of the tubular neighborhood  $N(\alpha)$  of  $\alpha$  in  $S$  is a Seifert surface of a Hopf link, and up to ambient isotopy, the Hopf link admits two minimal Seifert surfaces, and only one of them can give us  $S$  after gluing  $N(\alpha)$  back.

Since  $f$  sends the complement  $S \setminus N(\alpha)$  to  $S \setminus f(N(\alpha))$ , if  $f$  is orientation-reversing, then the two oriented Hopf links in Fig. 5.4 are ambient isotopic, but that is not possible by their linking numbers.  $\square$

## 6. REDUCIBLE HANDLEBODY LINKS

In this section, we show that Table 5 classifies, up to ambient isotopy and mirror image, all non-split, reducible  $(n, 1)$ -handlebody links up to six crossings (Theorem 1.3). We begin by considering the order-1 connected sum for handlebody links.

**6.1. Order-1 connected sum.** A handlebody-link-component pair  $(HL, h)$  is a handlebody link  $HL$  with a selected component  $h$  of  $HL$ .

**Definition 6.1 (Order-1 connected sum).** Let  $(HL_1, h_1)$  and  $(HL_2, h_2)$  be two handlebody-link-component pairs. Then their order-1 connected sum  $(HL_1, h_1)--(HL_2, h_2)$  is given by removing the interior of a 3-ball  $B_1$  (resp.  $B_2$ ) in  $\mathbb{S}^3$  with  $B_1 \cap \partial HL_1 = B_1 \cap \partial h_1$  (resp.  $B_2 \cap \partial HL_2 = B_2 \cap \partial h_2$ ) a 2-disk, and then gluing the resulting 3-manifolds  $\overline{\mathbb{S}^3 \setminus B_1}$ ,  $\overline{\mathbb{S}^3 \setminus B_2}$  via an orientation-reversing homeomorphism  $f : (\partial B_1, (\partial B_1) \cap h_1) \rightarrow (\partial B_2, (\partial B_2) \cap h_2)$ . We use  $HL_1--HL_2$  to denote the set of order-1 connected sums between  $HL_1, HL_2$  with all possible selected components.

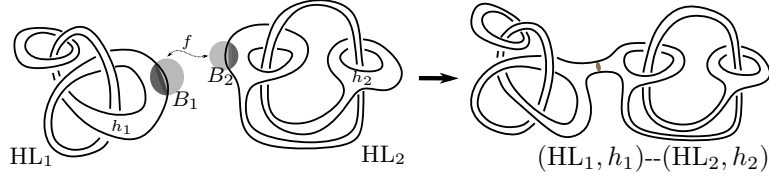


FIGURE 6.1. Order-1 connected sum of  $(HL_1, h_1)--(HL_2, h_2)$ .

The following generalizes the case of handlebody knots in [24, Theorem 2].

**Theorem 6.1 (Uniqueness).** Given a non-split, reducible  $(n, 1)$ -handlebody link  $HL$ , if  $HL \simeq (HL_1, h_1)--(HL_2, h_2)$ , and  $HL \simeq (HL'_1, h'_1)--(HL'_2, h'_2)$ , then  $(HL_i, h_i) \simeq (HL'_i, h'_i)$ ,  $i = 1, 2$ , up to reordering.

*Proof.* Note first that, since  $HL$  is non-split and reducible,  $HL_i, HL'_i$ ,  $i = 1, 2$ , are non-split, and  $\pi_1(\overline{\mathbb{S}^3 \setminus HL})$  is a non-trivial free product  $G_1 * G_2$ , where  $G_i$  is the knot group of  $HL_i$ ,  $i = 1, 2$ .

Let  $D$  and  $D'$  be the separating disks in  $\overline{\mathbb{S}^3 \setminus HL}$  given by the factorizations  $HL \simeq (HL_1, h_1)--(HL_2, h_2)$  and  $HL \simeq (HL'_1, h'_1)--(HL'_2, h'_2)$ , respectively. Suppose neither  $G_1$  nor  $G_2$  is isomorphic to  $\mathbb{Z}$ . Then, up to isotopy,  $D' \cap D = \emptyset$  by the innermost circle/arc argument.

Suppose one of  $G_i$ ,  $i = 1, 2$ , say  $G_1$ , is isomorphic to  $\mathbb{Z}$ , that is,  $HL_1$  is a trivial solid torus in  $\mathbb{S}^3$ . Then  $G_2$  must be non-cyclic, since  $n > 1$ . Let  $D_i$  be the disk bounded by the longitude of  $HL_1$ , and isotopy  $D, D_i$  such that the number  $n$  (resp.  $n_i$ ) of components of  $D' \cap D$  (resp.  $D' \cap D_i$ ) is minimized.

**Claim:**  $n_i = 0$ . Note first that the minimality implies that  $D' \cap D_i$  contains no circle components. Now, consider a tubular neighborhood  $N(D_i)$  of  $D_i$  in  $\overline{\mathbb{S}^3 \setminus HL}$  small enough such that  $\overline{N(D_i)} \cap D = \emptyset$  and  $\overline{N(D_i)} \cap D'$  are some disks, each of which intersects  $D_i^+$  (resp.  $D_i^-$ ) at exactly one arc on its boundary, where  $D_i^\pm \subset \partial \overline{N(D_i)}$  are proper disks in  $\overline{\mathbb{S}^3 \setminus HL}$  parallel to  $D_i$ . The claim then follows once we have shown that  $N(D_i)$  can be isotoped away from  $D'$ .

To see this, we construct a labeled tree  $\Upsilon$  from the complement of the intersection  $D' \cap D_i^\pm$  in  $D'$ , where  $D^\pm := D_i^+ \cup D_i^-$ . Regard each component of  $D' \setminus (D' \cap D^\pm)$  as a node in  $\Upsilon$ , and each arc in  $D' \cap D_i^\pm$  as an edge in  $\Upsilon$  connecting the two nodes representing the components of  $D' \setminus (D' \cap D^\pm)$  whose closures intersect at the arc. Since each arc in  $D' \cap D^\pm$  cuts  $D'$  into two,  $\Upsilon$  is a tree. The first two figures from the left in Fig. 6.2 illustrate the construction.



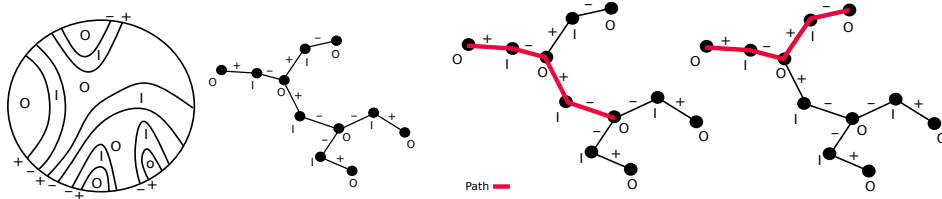


FIGURE 6.2.  $h(D_l)$  and  $\Upsilon$ .

We label nodes and edges of  $\Upsilon$  as follows: A node is labeled with  $I$  if the corresponding component of  $D' \setminus (D' \cap D^\pm)$  is inside  $N(D_l)$ ; otherwise the node is labeled with  $O$ . An edge of  $\Upsilon$  is labeled with  $+$  if the corresponding component of  $D' \cap D_l^\pm$  is in  $D_l^+$ ; otherwise, it is labeled with  $-$ .

The labeling on  $\Upsilon$  has the following properties: (a) adjacent nodes have different labels; (b) a node with label  $I$  is bivalent, and the two adjacent edges are labeled with  $+$  and  $-$ , respectively, whereas a node labeled with  $O$  could be multi-valent; (c) a one-valent node corresponds to an innermost arc in  $D'$ , and always has label  $O$ .

Consider a maximal path  $\Gamma \subset \Upsilon$  starting from a one-valent node and with the property that adjacent edges of  $\Gamma$  have different labels. Then the other end point of the path must be labeled with  $O$  and it is either a one-valent node of  $\Upsilon$  or a multi-valent node with all adjacent edges having the same label; the two figures from the right in Fig. 6.2 illustrate two possible maximal paths.

Without loss of generality, we may assume that the adjacent edge of the starting one-valent node of  $\Gamma$  is labeled with  $+$ . Denote the closure of the corresponding component of  $D' \setminus (D' \cap D^\pm)$  by  $D_\Gamma^s$ . Then  $\partial D_\Gamma^s$  bounds a disk  $T$  on  $\partial(\text{HL} \cup \overline{N(D_l)})$ . If  $T \cap D_l^- = \emptyset$ , then  $D_\Gamma^s \cap D = \emptyset$  and hence  $T \cap D = \emptyset$  by the minimality of  $n$ ; however, if it were the case, one could reduce  $n_l$  by isotopying  $D_l$  across the 3-ball bounded by  $D_\Gamma^s$  and  $T$ . Hence  $T$  must contain  $D_l^-$ . Since the adjacent edge of the starting node is labeled with  $+$ , adjacent edges of the end node of  $\Gamma$  in  $\Upsilon$  are labeled with  $-$ . Denote by  $D_\Gamma^e$  the closure of the component corresponding to the end node. Then  $\partial D_\Gamma^e$  bounds a disk in  $\partial(\text{HL} \cup \overline{N(D_l)})$  that is contained in  $T$  and has no intersection with  $D_l^+$ . Particularly,  $D_\Gamma^e \cap D = \emptyset$  by the minimality of  $n$ , and there is an arc in  $\partial D_\Gamma^e$  cutting a disk  $D''$  off  $T \setminus \overline{D_l^-}$  with  $\dot{D}'' \cap D' = D'' \cap D = \emptyset$ , so one can slide  $N(D_l)$  over  $D''$  (Fig. 6.3) to decrease  $n_l$ , a contradiction. Consequently,

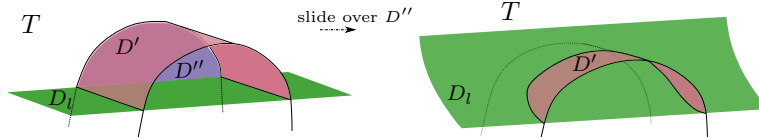


FIGURE 6.3

such a path  $\Gamma$  cannot exist, but this can happen only if  $\Upsilon$  is empty. The claim is thus proved. It implies that  $\text{HL}_1, \text{HL}'_1$  are trivial solid tori in  $\mathbb{S}^3$ , and  $\text{HL}_2, \text{HL}'_2$  are equivalent to  $\overline{N(D_l)} \cup \text{HL}$ . □

**6.2. Non-split, reducible handlebody links.** Table 5 lists all non-split, reducible  $(n, 1)$ -handlebody links obtained by performing order-1 connected sum on pairs of links  $(L_1, L_2)$  with crossing numbers  $(c_1, c_2)$  and  $c_1 + c_2 \leq 6$ . Since  $n > 1$ , one of  $L_1, L_2$ , say  $L_2$ , is a link with more than one component. The number in

TABLE 5. Reducible links with up to six crossings.

crossings	$c(L_1) + c(L_2)$	description	$ L_1--L_2 $
2 (1)	0 + 2	unknot -- Hopf	1
4 (4)	0 + 4	unknot -- L4a1	1
		unknot -- Hopf#Hopf	2
	2 + 2	Hopf -- Hopf	1
5 (4)	0 + 5	unknot -- Whitehead	1
		unknot -- Trefoil#Hopf	2
	3 + 2	trefoil -- Hopf	1
6 (17)	0 + 6	unknot -- L6ai, $i = 1, \dots, 5$	1
		unknot -- L6n1	1
		unknot -- L4a1#Hopf	3
		unknot -- (Hopf#Hopf)#Hopf	4
	2 + 4	Hopf -- L4a1	1
		Hopf -- Hopf#Hopf	2
	4 + 2	K4a1 -- Hopf	1

parentheses indicates the total number of inequivalent reducible handlebody links of the given crossing number. By Theorem 6.1, isotopy types of  $L_1$  and  $L_2$  with selected components determine the isotopy type of the resulting handlebody link  $L_1--L_2$ . Thus there are no duplicates in Table 5.

On the other hand, by Lemmas 4.1 and 4.3 and Theorem 3.7, minimal diagrams of non-split, reducible  $(n, 1)$ -handlebody links up to 6 crossings cannot have  $k$ -connectivity,  $k > 1$ . This shows the completeness of Table 5.

In particular, every non-split, reducible  $(n, 1)$ -handlebody link in Table 5 admits a minimal diagram with 1-connectivity; thus we postulate the following conjecture.

**Conjecture 6.2.** *Every non-split, reducible handlebody link admits a minimal diagram with 1-connectivity.*

Not every minimal diagram of a reducible handlebody link has 1-connectivity. By Theorem 6.1, Conjecture 6.2 implies the additivity of the crossing number (Conjecture 6.3), a reminiscence of a one-hundred years old problem in knot theory.

**Conjecture 6.3.** *If  $(HL_1, h_1)--(HL_2, h_2)$  is a  $(n, 1)$ -handlebody link, then*

$$c((HL_1, h_1)--(HL_2, h_2)) = c(HL_1) + c(HL_2). \quad (6.1)$$

#### ACKNOWLEDGEMENTS

The first author benefits from the support of the GNAMPA (Gruppo Nazionale per l'Analisi Matematica, la Probabilità e le loro Applicazioni) of INdAM (Istituto Nazionale di Alta Matematica). The second author benefits from the support of the Swiss National Science Foundation Professorship grant PP00P2.179110/1. The fourth author is supported by National Center of Theoretical Sciences.

#### REFERENCES

- [1] I. Bertuccioni, *A Topological Puzzle*, Amer. Math. Monthly **110** (2003), 937–939.
- [2] G. Bellettini, M. Paolini, Y.-S. Wang, *Numerical irreducibility criteria for handlebody links*, arXiv:2002.05974 [math.GT].
- [3] J. Botermans, P. Van Delft, *Creative Puzzles of the World*, Abrams, New York, 1975.
- [4] M. Brown, *Locally Flat Imbeddings of Topological Manifolds* Ann. Math., Second Series, **75**, (1962), 331–341.
- [5] Chongchitmate, Wutichai, Ng, Lenhard *An atlas of Legendrian knots*, Exp. Math. **22** (2013), no. 1, 26–37.

- [6] I. A. Grushko, *On the bases of a free product of groups*, Matematicheskii Sbornik, **8** (1940), 169–182.
- [7] M. W. Hirsch, B. Mazur, *Smoothings of Piecewise Linear Manifolds*, (AM-80), Princeton University Press, Princeton, NJ, (1974).
- [8] J. Hoste, M. Thistlethwaite, J. Weeks *The first 1,701,936 knots*, Math. Intelligencer **20** (1998), 33–48.
- [9] A. Ishii, *Moves and invariants for knotted handlebodies*, Algebr. Geom. Topol. **8** (2008), 1403–1418.
- [10] A. Ishii, K. Kishimoto, H. Moriuchi, M. Suzuki, *A table of genus two handlebody-knots up to six crossings*, J. Knot Theory Ramifications **21** (2012).
- [11] A. Ishii, K. Kishimoto, and M. Ozawa, *Knotted handle decomposing spheres for handlebody-knots*, J. Math. Soc. Japan **67** (2015), 407–417.
- [12] L. H. Kauffman, *Invariants of graphs in three-space*, Trans. Amer. Math. Soc. **311** (1989) (2), 679–710.
- [13] T. Kitano, M. Suzuki, *On the number of  $SL(2, \mathbb{Z}/p\mathbb{Z})$ -representations of knot groups* J. Knot Theory Ramifications **21** (2012).
- [14] Y. Koda, M. Ozawa, with an appendix by C. Gordon, *Essential surfaces of non-negative Euler characteristic in genus two handlebody exteriors*, Trans. Amer. Math. Soc. **367** (2015), no. 4, 2875–2904.
- [15] P. Melvin, *A Topological Menagerie*, Amer. Math. Monthly, **113** (2006) 348–351.
- [16] A. Mizusawa, *Linking numbers for handlebody-links*, Proc. Japan Acad. **89**, Ser. A (2013), 60–62.
- [17] H. Moriuchi, *An enumeration of theta-curves with up to seven crossings* J. Knot Theory Ramifications **18** (2009), 67–197.
- [18] H. Moriuchi, *A table of handcuff graphs with up to seven crossings* OCAMI Studies Vol 1. Knot Theory for Scientific objects (2007) 179–300.
- [19] H. Moriuchi, *A table of  $\theta$ -curves and handcuff graphs with up to seven crossings* Adv. Stud. Pure Math. Noncommutativity and Singularities: Proceedings of French–Japanese symposia held at IHES in 2006, J.-P. Bourguignon, M. Kotani, Y. Maeda and N. Tose, eds. (Tokyo: Mathematical Society of Japan, 2009), 281–290.
- [20] J. Munkres, *Elementary Differential Topology*, (AM-54), Princeton University Press, Princeton, NJ (1966).
- [21] M. Paolini, Appcontour. Computer software. Vers. 2.5.3. Apparent contour. (2018) <<http://appcontour.sourceforge.net/>>.
- [22] C. P. Rourke, B. J. Sanderson, *Introduction to Piecewise-Linear Topology*, Springer-Verlag, Berlin-New York, (1982).
- [23] S. Suzuki, *On surfaces in 3-sphere: prime decompositions*, Hokkaido Math. J. **4** (1975), 179–195.
- [24] Y. Tsukui, *On a prime surface of genus 2 and homeomorphic splitting of 3-sphere*, The Yokohama Math. J. **23** (1975), 63–75.
- [25] H. Whitney, *Congruent graphs and the connectivity of graphs*, Am. J. Math. **54** (1932), 150–168.
- [26] D. N. Yetter, *Category theoretic representations of knotted graphs in  $S^3$* , Adv. Math. **77** (1989) 137–155.

## APPENDIX A. OUTPUT OF THE CODE

**A.1. Minimal diagrams from the code.** The software code used in the paper exhaustively enumerates 3-edge-connected plane graphs with two trivalent vertices and  $q$  quadrivalent vertices,  $0 < q \leq 6$ , without double arcs that form a non-bigon. Note that the trivial theta curve is the only 3-edge-connected plane graph without quadrivalent vertices. The output of the code is examined and summarized in Table 3, while the detailed list is available on <http://dmf.unicatt.it/paolini/handlebodylinks/>, where each plane graph is described by its adjacent matrix together with a fixed ordering (clockwise or counterclockwise) of the edges adjacent to every vertex, as determined by the planar embedding.

**A.1.1. Four crossings or less.** In Table 6, we analyze the output of the code up to 4 quadrivalent vertices, where the column “quad. v.” lists the number of quadrivalent vertices and “ref. no.” the reference number of each plane graph in the output of the code. The column “induced diagrams” describes minimality of diagrams induced

by each plane graph. Most induced diagrams are not minimal, and we record those that are and their isotopy types as special graphs or handlebody links, up to mirror image. Up to 4-crossings, no IH-minimal diagram with more than one component is found.

TABLE 6. Diagrams with up to 4 crossings.

quad. v.	ref. no.	induced diagrams
1	none	none
2	#1	R-minimal; G2 <sub>1</sub> in Table 4; not IH-minimal
3	#1,	not R-minimal
	#2,#3	R-minimal; G3 <sub>2</sub> in Table 4; not IH-minimal
4	#1,#2	IH-minimal; G4 <sub>1</sub> in Table 4
	#3	R-minimal; G3 <sub>2</sub> in Table 4; not IH-minimal
	#4, #8	R-minimal; G4 <sub>2</sub> in Table 4; not IH-minimal
	#5, #6, #7	R-minimal; G4 <sub>3</sub> in Table 4; not IH-minimal
	#9	R-minimal; G4 <sub>4</sub> in Table 4; not IH-minimal
	#10	R-minimal; G4 <sub>5</sub> in Table 4; not IH-minimal

TABLE 7. Diagrams with 5 crossings.

ref. no.	description
#6, #11, #14	not R-minimal
#22, #26, #35	not IH-minimal
#36	not IH-minimal
#37	not R-minimal

A.1.2. *Five and six crossing cases.* In the 5 crossings case, the code finds 8 plane graphs with more than one components, out of a total of 37 planar embeddings. Table 7 records the analysis for their induced diagrams; none of them gives IH-minimal diagrams. In the 6 crossing case, out of 181 plane graphs, 37 induces diagrams with more than one components. Table 8 records the minimality of their induced diagrams.

Fig. A.1 exemplifies how the analysis is done. Fig. A.1a shows how the diagrams induced by Plane Graph #5 are equivalent to those by #161 and #165 in the case of 6 crossings, and Fig. A.1b explains non-minimality of diagrams induced by Plane Graphs #168, #169, #170, #171.

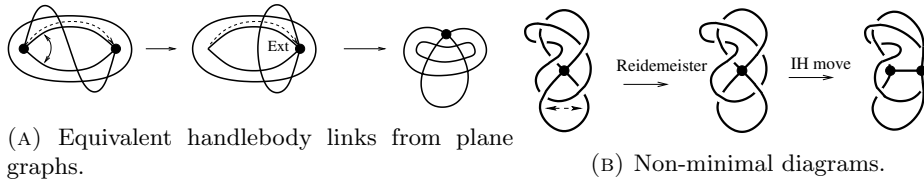
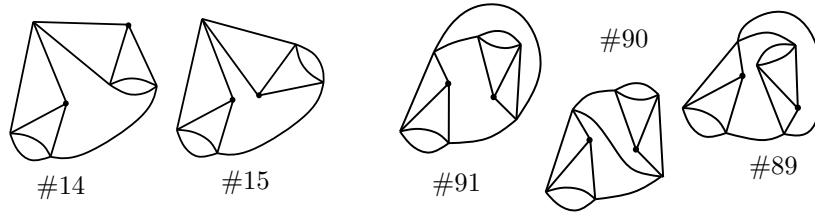


FIGURE A.1.

TABLE 8. Diagrams with 6 crossings.

ref. no.	description
#5	$6_1$ in Table 1
#15, #22, #34, #45, #54	not R-minimal
#56	$6_1$ in Table 1
#60	$6_2$ in Table 1
#70	$6_3$ in Table 1
#73	not R-minimal
#83	$6_2$ in Table 1
#84	$6_1$ in Table 1
#86, #91, #92, #93	not R-minimal
#104, #105, #114, #117, #123	not IH-minimal
#134, #135, #137, #144	not IH-minimal
#161, #165	$6_1$ in Table 1
#168, #169, #170, #171	not IH-minimal
#175	$6_9$ in Table 1
#176	not IH-minimal
#177	not R-minimal
#179, #180	not IH-minimal
#181	$6_9$ in Table 1



(A) Five-quadrivalent-vertex graph. (B) Six-quadrivalent-vertex graph.

FIGURE A.2. Inequivalent planar embeddings.

A.1.3. *Inequivalent planar embeddings.* As a side remark, Fig. A.2 illustrates two examples of abstract graphs with inequivalent planar embeddings: one with five quadrivalent vertices and the other with six. Note that the abstract graphs have 2-vertex-connectivity, consistent with the Whitney uniqueness theorem [25].

DIPARTIMENTO DI INGEGNERIA DELL'INFORMAZIONE E SCIENZE MATEMATICHE, UNIVERSITÀ DI SIENA, 53100 SIENA, ITALY, AND INTERNATIONAL CENTRE FOR THEORETICAL PHYSICS ICTP, MATHEMATICS SECTION, 34151 TRIESTE, ITALY  
*E-mail address:* [bellettini@diism.unisi.it](mailto:bellettini@diism.unisi.it)

CALIFORNIA INSTITUTE OF TECHNOLOGY AND AMAZON WEB SERVICES, PASADENA CA, UNITED STATES (WORK DONE WHILE AT UNIVERSITY OF FRIBOURG, DEPARTMENT OF MATHEMATICS, 1700 FRIBOURG, SWITZERLAND)  
*E-mail address:* [paolini@caltech.edu](mailto:paolini@caltech.edu)

DIPARTIMENTO DI MATEMATICA E FISICA, UNIVERSITÀ CATTOLICA DEL SACRO CUORE, 25121 BRESCIA, ITALY  
*E-mail address:* [maurizio.paolini@unicatt.it](mailto:maurizio.paolini@unicatt.it)

NATIONAL CENTER FOR THEORETICAL SCIENCES, MATHEMATICS DIVISION, TAIPEI 106, TAIWAN  
*E-mail address:* [yisheng@ncts.ntu.edu.tw](mailto:yisheng@ncts.ntu.edu.tw)